Conversion of the *Escherichia coli* Cytochrome b_{562} to an Archetype Cytochrome *b*: A Mutant with Bis-Histidine Ligation of Heme Iron†

Sam Hay* and Tom Wydrzynski

Photobioenergetics, Research School of Biological Sciences, The Australian National University, Canberra ACT 0200, Australia

Received April 19, 2004; Revised Manuscript Received July 1, 2004

ABSTRACT: A mutant of the *Escherichia coli* cytochrome b_{562} has been created in which the heme-ligating methionine (Met) at position 7 has been replaced with a histidine (His) (M7H). This protein is a double mutant that also has the His 63 to asparagine (H63N) mutation, which removes a solvent-exposed His. While the H63N mutation has no measurable effect on the cytochrome, the M7H mutation converts the atypical His/Met heme ligation in cytochrome b_{562} to the classic cytochrome *b*-type bis-His ligation. This mutation has little effect on the K_d of heme binding but significantly reduces the chemical and thermal stability of the mutant cytochrome relative to the wild type (wt). Both proteins have similar absorbance (Abs) and electron paramagnetic resonance (EPR) properties characteristic of 6-coordinate low-spin heme. The Abs spectra of the oxidized and reduced bis-His cytochrome are slightly blue-shifted relative to the wt, and the α Abs band of ferrous M7H mutant is unusually split. The M7H mutation decreases the midpoint potential of the bound heme by 260 mV at pH 7 and considerably alters the pH dependence of the E_m, which becomes dominated by a single $pK_{red} = 6.8$.

Cytochrome b_{562} is a small, soluble four-helix-bundle protein with a single *b*-type heme cofactor originally described by Itagaki and Hagar (*1*). This protein is found in the periplasm of *Escherichia coli* and, while its postulated role is in electron transfer, no physiological partners nor biological function have been assigned to it. Cytochrome b_{562} is quite enigmatic because it is the only soluble cytochrome without a covalently attached heme and one of only two known *b*-type cytochromes with methionine/histidine (Met/His)[1] heme iron ligation (the other protein being the fungal extracellular flavocytochrome cellobiose dehydrogenase [rCDH) (*2*)]. Cytochrome b_{562} has been well-characterized both structurally (*3*, *4*) and biophysically (for example, see refs *5*, *6*, *7*, and *8*). This makes cytochrome b_{562} a good candidate for the study of protein−porphyrin binding interactions. Upon binding to a protein, heme forms axial ligands with one or two protein side chains. The amino acid side chains of His, Met, lysine, asparagine, tyrosine, proline, and cysteine are able to act as such ligands forming nitrogen−, sulfur−, or oxygen−iron bonds. The amino terminus has also been shown to act as a ligand. This bonding has a major role in regulating the properties of the ligated heme as well as potentially playing a significant role in the stabilization of the heme−protein complex. In the cytochromes, bis-His and Met/His ligation are much more common than the other forms of ligation, where bis-His ligation predominates in the *b*-type cytochromes and Met/His ligation is generally found in the *c*-type cytochromes. The *E. coli* cytochrome b_{562} has atypical Met/His ligation, and this work describes the mutation of of the iron-ligating Met to a His, forming a protein capable of bis-His ligation of the heme iron. Heme reconstitution, optical spectroscopy, guanidine and thermal denaturation, redox potentiometry, low-temperature electron paramagnetic resonance (EPR), and molecular modeling have been used to characterize this mutant protein relative to the wild type (wt).

MATERIALS AND METHODS

Cloning and Mutagenesis. The *CybC* gene encoding cytochrome b_{562} was cloned from *E. coli* strain BL21 (Novagen Inc.). The primers were designed not to amplify the region encoding the N-terminal periplasmic signaling sequence and had the following forward and reverse sequences, respectively: GGTATTGAGG GTCGCATGGC TGATCTTGAA GACAATATGG AAACC and AGAGGAGAGT TAGAGCCTCA TTAACGATAC TTCTGGTGAT AGGCG. The gene was ligated into the Novagen vector pET-30 Xa/LIC, which encodes an N-terminal His tag in-frame. These primers also inserted a Met at the N terminus of the cytochrome (the numbering referred to here keeps with convention, and thus, this Met is at position 0 and not 1). Once ligated, the plasmid was transformed into NovaBlue (Novagen Inc.) and all constructs were screened by sequencing. *E. coli* strain BL21 pLysS DE3 (Novagen) was then transformed with this vector for protein expression. First, to eliminate any possibility of nonspecific heme binding to the protein, the H63N mutant was made by site-directed mutagenesis of the cloned *CybC* gene using the forward and reverse primers, respectively: GATTTCCGCA ACGGTTTCGA C and GTCGAAACCG TTGCGGAAAT C. The M7H

† This work was supported in part by Australian Research Council Discovery Project Grant DP045021 and an Australian National University Graduate School Scholarship to S.H.

* To whom correspondence should be addressed. Phone: +61 (0)2 6125 2386. Fax: +61 (0)2 6125 8056. E-mail: hay@rsbs.anu.edu.au.

[1] Abbreviations: Abs, absorbance; bis-Im-heme, bis-imidazole-ligated hemin in solution; CD, circular dichroism; His, histidine; HS, high spin; LS, low spin; Met, methionine; SHE, standard hydrogen electrode; wt, wild type.

10.1021/bi0492298 CCC: $30.25
Published on Web 12/02/2004

mutation was then created by subsequent mutagenesis of the H63N mutant using the forward and reverse primers, respectively: CTTGAAGACA ATCATGAAAC CCTCAAC and GTTGAGGGTT TCATGATTGT CTTCAAG. All molecular biology enzymes and reagents were from New England Biolabs, Roche, Novagen, or Qiagen.

Protein Expression and Purification. The recombinant proteins were expressed and initially purified by imobilized metal-affinity chromatography with Fractogel (Novagen) essentially as described previously (*9*). The His-tagged protein generally eluted in a volume of about 50−80 mL and was dialyzed against 4 L of water overnight to remove the imidazole. It was then concentrated in a Centriprep YM-10 (Millipore) filtration unit (typically to a final volume of 10−20 mL). The buffer was adjusted to 20 mM Tris, 100 mM NaCl, and 5 mM $CaCl_2$ at pH 8.0, and the protein was incubated with 30 units of the site-specific protease Factor Xa (Novagen) at 37 °C with gentle shaking for 24−48 h. The cleavage was monitored by sodium dodecyl sulfate−polyacrylamide gel electrophoresis (SDS−PAGE). Once cleavage was complete, the protein was loaded onto a 5 cm diameter column containing Ni-NTA resin (QIAGEN) pre-equilibrated with 50 mM Tris and 100 mM NaCl at pH 8.0. The flow-through containing the cytochrome was collected and again concentrated in a Centriprep YM-10.

Generally, at this stage, the protein was considered to be pure, because only one band was visible on an overloaded SDS−PAGE gel stained with Coomassie brilliant blue. The apparent size of the cytochrome on the gel was consistent with expectations, and N-terminal sequencing confirmed cleavage of the N-terminal His tag/linker. If contamination was present, then the protein was dialyzed against 10 mM potassium phosphate at pH 7.0. This was loaded onto a DEAE Sepharose (Amersham Pharmacia Biotech) column and eluted with 50 mM NaCl and 10 mM potassium phosphate at pH 7.0. This was sufficient to remove any remaining contaminants.

When necessary, heme was removed from the holoproteins by the method of Teale (*10*). The apoprotein was reconstituted with freshly prepared hemin chloride or other porphyrins by standard literature methods (*11*, *12*), by the slow addition of <1 μM aliquots of porphyrin to the apoprotien with constant mixing. K_d values for heme binding were determined by the careful titration of small aliquots of hemin or hemin and sodium dithionite into a solution of the apoprotein with the extent of binding monitored by heme absorbance (Abs). Titrations were fit to

$$\Delta\text{Abs} = \epsilon_b[\text{bound}] + \epsilon_s[\text{unbound}]$$

$$[\text{bound}] = \frac{1}{2}\left(([E_0] + [L] + K_d) - \sqrt{([E_0] + [L] + K_d)^2 - 4([E_0][L])}\right)$$

$$[\text{unbound}] = [L] - [\text{bound}] \quad (1)$$

where ΔAbs is the change in Abs at a wavelength of interest (e.g., Soret maxima), ϵ_b and ϵ_s are the absorption coefficient of protein-bound heme and heme in solution, respectively, at this wavelength, $[E_0]$ is the protein concentration, and $[L]$ is the total heme concentration. Typically, $[E_0]$ was determined by titration of 200 nM aliquots of hemin into >2 μM apoprotein ($[E_0] \gg [L] \gg K_d$), and K_d was determined by titration of 10 or 100 nM aliquots of hemin or hemin and dithionite into known concentrations of apoprotein at ~10−20× the aliquot concentration. For circular dichroism (CD) and denaturation experiments, protein was reconstituted with equimolar hemin, but for other experiments, generally, a total hemin concentration no greater than 80% of the protein was used to minimize unbound heme. Hemin chloride was purchased from Sigma and free-base protoporphyrin IX from Porphyrin Products (Frontier Scientific). Both porphyrins were used as supplied and only fresh stock solutions in dimethylsulfoxide where used. Hemin concentration was determined by $\epsilon_{385\ nm} = 58.4\ mM^{-1}$ in water.

Chromatography and Denaturation. Size-exclusion chromatography was performed on two Protein Pak 300sw columns (Waters) at 1 mL min^{-1} in 10 mM potassium phosphate at pH 7.0, with detection at 220 nm. The column was calibrated using insulin (5.7 kDa), ribonuclease S (11.5/2.2 kDa), horse heart cytochrome *c* (12.3 kDa), lysozyme (14.4 kDa), myoglobin (17 kDa), chymotrypsenogen A (25.7 kDa), pepsin (36 kDa), catalase (60 kDa), and bovine serum albumin (67 kDa).

Guanidine denaturation was performed by incubation of oxidized cytochrome in guanidine for at least 1 h at 20 °C before measurement. The sample also contained 50 mM potassium phosphate and 100 mM KCl at pH 7.0. The degree of denaturation was followed by bound heme Soret Abs and fit to a two-state transition of the form: fraction folded = $1/[1 + \exp(-(\Delta G^{H_2O} - m[\text{Gdn}])/RT)]$, according to the method of Pace (*13*). Thermal denaturation was performed with the aid of a circulating waterbath. The temperature was increased in 2−5 °C increments, and the samples were equilibrated for >5 min before measurement. The extent of unfolding was determined by Soret Abs for holoproteins or second-derivative UV Abs for the apoprotein. The data were corrected with first-order baselines, and ΔH and T_M were determined from the derivative of the data in Figure 3. ΔG was calulated from this using the Gibbs−Helmholtz equation

$$\Delta G = H_{vH}(1 - T/T_M) - \Delta C_p(T_M - T - T\ln(T/T_M)) \quad (2)$$

with ΔC_p values of 0.56 for apoprotein and 0.92 for holoprotien, which were determined previously for apo- and holo-wt cytochrome b_{562}, respectively (*14*).

Spectroscopy. CD spectroscopy was performed on a ISA Jobin Yvon CD 6 spectropolarimeter (Instruments S. A. Inc.) at room temperature using a 0.1 or 1 cm quartz cell for the UV and Soret region, respectively. Abs measurements were made on a Varian Cary 300 spectrophotometer with 1 cm path-length cuvettes.

EPR measurements were performed on a Bruker ESP 300E spectrometer at 9.4 GHz. Instrument details are given in the Figure 4 caption. All measurements were made at 10 K, and 20% glycerol was used as a cryoprotectant in all samples. When necessary, g_x values were calculated by the method described in ref *17* by $g_x^2 + g_y^2 + g_z^2 - g_xg_y - g_xg_z + g_yg_z + 4g_x - 4g_y - 4g_z = 0$. The ligand field parameters V (rhombic splitting) and Δ (tetragonal splitting) were calculated using the method described in ref *18* from the 3 low-spin (LS) g tensors. These were calculated in units of λ (spin−orbit-coupling constant), where $V/\lambda = g_x/(g_z + g_y) + g_y/(g_z - g_x)$

Table 1: Abs, EPR, and Redox Properties of wt, H63N, and M7H Cytochrome b_{562} and bis-Im-heme

		Abs maxima (nm)			
	ligation[a]	oxidized	reduced	EPR (g_z, g_y, g_x)	E_{m7}[b]
wt cyt b_{562}	H/M	418, 529, 558 (i)	427, 531, 562 (i)	3.04, 2.18 (ii)	+189 (iv)
H63N	H/M	418, 530, 560	427, 531, 561	3.04, 2.18, 1.40[c]	+187
M7H	H/H	415, 537, 566	426, 531, 558/561[d]	3.02, 2.20, 1.41[c]	−73
bis-Im-heme	Im/Im	409, 534, 563	421, 526, 556	3.02, 2.24,1.51 (v)	−143

[a] Heme ligation by bis-His (H/H), His/Met (H/M), or bis-imidazole (Im/Im). [b] The midpoint potentials were measured in millivolts versus the SHE at pH 7. [c] These g_x values were calculated, see text for details. [d] The α band of M7H is partially split. Additional data taken from (i) Itagaki and Hagar (*1*), (ii) Walker et al. (*17*), (iii) Barker et al. (*46*), and (iv) Peisach et al. (*39*).

and $\Delta/\lambda = g_x/(g_z + g_y) + g_z/(g_y - g_x) - 1/2V/\lambda$, with $g_z > g_y > g_x$.

Redox potentiometry was performed essentially by the method of Dutton (*15*) in an anaerobic cell continuously flushed with nitrogen. The mediators (10 μM) used were a mixture of some or all of the following depending on the potential scanned: 1,4-benzoquinone, diamino duroquinone, phenazine methosulfate, phenazine ethosulfate, duroquinone, 1,2-naphthoquinone, 1,4-naphthoquinone, trimethyl hydroquinone, juglone, and riboflavin-5′-monophosphate. The titrations were performed in an oxidizing direction by the addition of ferricyanide and in the reducing direction with buffered sodium dithionite. The samples were in 100 mM KCl and buffered with 50 mM sodium acetate, potassium phosphate, or Tris, as required. Bis-imidazole-ligated heme was prepared by the addition of 100 mM imidazole to fresh-stirred hemin in solution weakly buffered to pH 8. The concentration of hemin was kept below ~20 μM to reduce aggregation. The sample was then buffered with 50 mM potassium phosphate, and the pH was adjusted to 7.0. The redox titration data was fit to a single Nernst curve of the form: fraction reduced $= 1/[1 + 10^{(E-E_m)/(59/n)}]$, where E is the solution redox potential in units of millivolts versus the standard hydrogen electrode (SHE). The data were fit with n as a free variable, yet it always fit with n in the range of ~0.9−1.1.

RESULTS

Protein Expression and Purification. wt cytochrome b_{562} has a solvent-exposed His residue at position 63, which we replaced with an asparagine, creating the H63N mutant. Both the H63N and M7H proteins also have an N-terminus Met as a result of the expression plasmid used. This additional Met is expected to be >15 Å from the heme iron, and we have seen no evidence for it playing any role in heme binding. The rationale for the H63N mutation was to prevent the adventitious binding of heme to this solvent-exposed residue upon reconstitution of the apoprotein. Additionally, His 63 has been mutated in cytochrome b_{562} by other groups (*16*) without problems. The Met and H63N mutations did not effect the absorption, redox, or EPR properties of the protein relative to the wt (see Table 1) and had no measurable effect on the chemical stability of the protein. M7H is a double mutant that also contains the H63N mutation. Recombinant cytochrome b_{562} and the H63N and M7H mutants were overexpressed in *E. coli* using the pET-30 Xa/LIC system. This yielded pure cytochrome up to about 50 mg of pure protein per liter of culture, and typically, about 20−30% of the protein contained bound heme. It is interesting to note that the cytochrome was expressed with an N terminus consisting of a ~4-kDa fused His tag/linker in place of the usual periplasmic signaling sequence, yet heme was still incorporated into the recombinant protein to a level of over 1 μmol of heme per liter of culture, which resulted in distinctive red/pink-colored *E. coli* after several hours of protein expression. When necessary, the heme was removed from the purified cytochromes by the method of Teale (*10*), and reconstitution of the apoproteins with hemin resulted in indistinguishable characteristics relative to those of the endogenous heme-containing cytochromes.

Gel-Filtration Chromatography. The apo form of M7H elutes from a size-exclusion gel-filtration column with an apparent mass of 23.6 kDa. Hemin-reconstituted M7H eluted slightly later with an apparent mass of 22.9 kDa. This reduction in apparent mass upon hemin-binding is consistent with reports for the wt protein (*20*) and, on this column, the wt apo- and ferricytochrome elute with apparent masses of 20.1 and 19.9 kDa, respectively. The slightly later elution time of M7H relative to the wt is consistent with M7H having a more disordered or less compact fold. It was previously noted that cytochrome b_{562} has a larger than expected apparent molecular weight (~18 kDa) relative to that of the molecular weight of the cytochrome of 12.3 kDa (*20*), and the authors postulated that this is due to the highly asymmetric shape of the protein. Despite the large apparent size of apo and holo M7H, the elution times of these proteins are independent of the protein concentration (<1−500 μM) and elute much later than a covalently dimerized cytochrome b_{562} variant (Hay, unpublished data), confirming the monomeric state of the M7H protein.

Absorption Spectroscopy. The Abs spectra of H63N and wt cytochrome are indistinguishable (data not shown). The Abs spectra of oxidized and reduced H63N and M7H are shown in Figure 1, and the peak maxima are listed in Table 1. The spectra are all typical of LS cytochromes. The Soret band is blue-shifted by 3 and 1 nm, respectively, in ferri and ferrous M7H, relative to H63N. Additionally, ferrous M7H auto-oxidizes very quickly. The α band of reduced M7H is broadened and somewhat split relative to wt and also shows a decreased intensity from 32 to 24 mM^{-1} cm^{-1}. This is shown in the inset of Figure 1 relative to that of H63N. A weak charge-transfer band is visible in the wt (and H63N) cytochrome at about 720 nm at pH 7 but is not visible in M7H (data not shown). This Abs is thought to arise from the Met (*7*) S → Fe charge transfer and thus is not expected in the bis-His variant (*19*). The careful titration of hemin into apo M7H yielded binding with a K_d too small to measure (<1 nM), while the titration of heme yielded a K_d value of 20 ± 3 nM (not shown). Similar titrations performed with apo H63N give a K_d value of 13 ± 3 nM for hemin binding

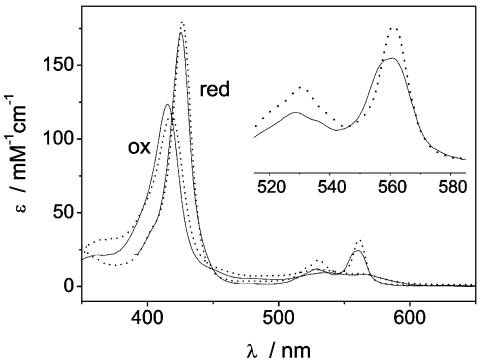

FIGURE 1: Abs spectra of oxidized and reduced H63N (···) and M7H (—) mutants of cytochrome b_{562}. The inset shows the α and β bands of the ferrous cytochromes and highlights the splitting of the M7H α band. The peak postions are given in Table 1.

Table 2: Heme-Binding Constants

protein	K_d[a] (nM) Fe^{III}−heme	K_d[a] (nM) Fe^{II}−heme	$\Delta\Delta G$[b] (kcal mol^{-1})
H63N	13 ± 3	2.8 ± 0.6	0.9
M7H	<1	20 ± 3	>−1.7

[a] Determined by optical titrations fit to eq 1 as described in the text. [b] Difference in the energetics of Fe^{III}−heme binding relative to Fe^{II}−heme binding to each protein.

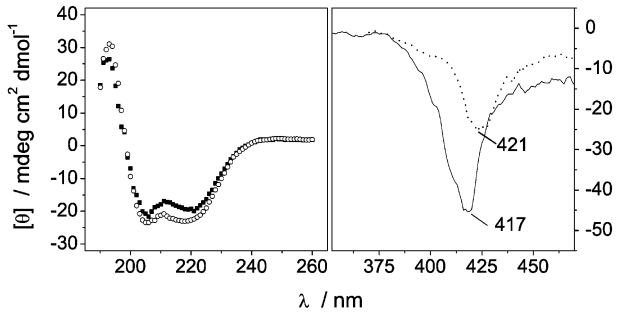

FIGURE 2: CD spectra. Left, apo- (■) and hemin-reconstituted (○) M7H. Right, the Soret region of oxidized (—) and reduced (···) holo M7H. The protein concentration was 5 μM (far UV) or 20 μM in 10 mM potassium phosphate and 100 mM KCl at pH 7.0 and room temperature.

and K_d value of 2.8 ± 0.6 nM for heme (see Table 2). Hemin-binding to wt cytochrome b_{562} was measured by calorimetry to have a K_d of 9 nM (*7*), and agreement with the value obtained for H63N further suggests that the N-terminus Met and H63N mutations have little effect on cytochrome b_{562}. Interestingly, both the wt and M7H apoproteins bind a free-base protoporphyrin IX with micromolar affinity, shifting the Soret Abs from 393 to 408 nm despite the lack of any metal ligation (data not shown).

CD. The far-UV CD spectra of the apo- and hemin-reconstituted M7H are shown in Figure 2. Upon fitting of the CD spectra, the helical content of the apo form of M7H was estimated to be 54%. This is similar to the value of 57% reported for wt apocytochrome (*20*). Upon reconstitution of M7H with hemin, there was a small increase in helicity to ~60%, and this was sensitive to buffer conditions, requiring 100 mM KCl for maximal increase. This contrasts with the increase in the helicity of wt cytochrome to 82% upon hemin binding (*20*). The $\theta_{222}/\theta_{208}$ ratios of the apo- and ferri-M7H mutant are 1.02 and 1.03, respectively, indicating these proteins have a coiled-coil conformation (*21*), but this is less

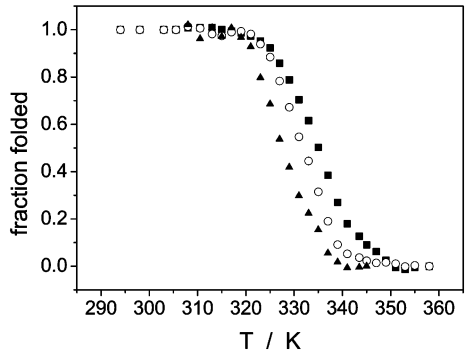

FIGURE 3: Thermal denaturation of apo M7H (▲), measured by second-derivative UV Abs, and ferrous (○) and ferri (■) M7H measured by the loss of the bound heme Soret Abs. Samples were in 100 mM KCl and 50 mM potassium phosphate at pH 7. The thermodynamic parameters obtained are given in Table 3.

Table 3: Thermal Denaturation Parameters

protein	T_M (°C)	ΔH[a] (kcal mol^{-1})	ΔG[b] (kcal mol^{-1})
apo M7H	54.3 ± 0.3	44.5 ± 5	3.6
ferrous M7H	58.5 ± 0.3	56.4 ± 4	4.4
ferri M7H	61.4 ± 0.3	55.2 ± 3	4.4
apo wt[c]	54.04 ± 0.02	47.4 ± 2.8	3.9
holo wt[c]	66.99 ± 0.15	104.2 ± 2.5	11.3

[a] The enthalpy of unfolding, ΔH, from this work was determined by the method described in ref *47*. [b] The free energy of unfolding, ΔG, was estimated using the Gibbs−Helmholtz equation (eq 2) with ΔC_p = 0.56 kcal mol^{-1} K^{-1} for apoproteins and ΔC_p = 0.92 kcal mol^{-1} K^{-1} for holoproteins (*14*). [c] Additional data taken from Robinson et al. (*14*) were measured by differential-scanning calorimetry and are similar to those reported by Feng and Sligar (*20*) as measured by the loss of Abs or CD.

so than for the apo-H63N protein, which has a $\theta_{222}/\theta_{208}$ ratio of 1.14. The Soret-region CD of ferri and ferrous M7H confirmed that, despite only a small increase in helicity, the heme was bound to M7H in these experiments. These spectra are also shown in Figure 2 and are similar to those reported for wt cytochrome b_{562} (*22*).

Denaturation. The stability of the ferri-M7H and ferri-H63N proteins was investigated using guanidine denaturation at pH 7.0. The guanidine-induced unfolding of the ferri-cytochromes was monitored by loss of bound heme (data not shown). It has been shown that heme loss occurs concurrently with the loss of the secondary structure in wt cytochrome b_{562} (*20*), and this was assumed to be the case for H63N and M7H. The energetics of the unfolding process were fit to a two-state linear denaturant binding model (*13*) with a ΔG^{H_2O} of 7.0 for ferri-wt cytochrome b_{562} (with N-terminus Met), 6.8 kcal mol^{-1} for ferri H63N and 4.3 kcal mol^{-1} for ferri M7H. A ΔG^{H_2O} of 6.6 kcal mol^{-1} has previously been reported for the wt ferricytochrome denatured in urea by Feng and Sligar (*20*), who also determined a ΔG^{H_2O} of 3.2 kcal mol^{-1} for the apocytochrome. The stabilization of heme-binding to M7H was further investigated by thermal denaturation, which is shown in Figure 3 for the apo-, ferrous-, and ferri-M7H proteins. This is compared to data from similar experiments for the wt protein (*14, 20*) in Table 3.

EPR Measurements. The low-temperature X-band EPR spectra of ferri H63N and ferri M7H are shown in Figure 4. The features at $g \sim 3$ and $g \sim 2.2$ arise from LS heme. The

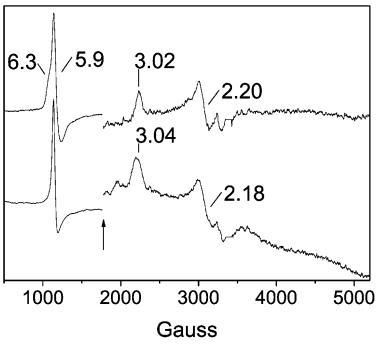

FIGURE 4: X-band EPR spectra at 10 K of ferri M7H (top) and ferri H63N (bottom). The portion of the spectra to the right of the arrow is magnified 5×. The proteins were at 100 μM concentration in 50 mM potassium phosphate, 100 mM KCl, and 20% glycerol at pH 7. Spectra were recorded at a microwave power of 2 mW and a modulation amplitude of 10 G. The g values mentioned in the text are marked.

sharp feature at $g = 5.9$ is a high-spin (HS) heme and accounts for less than 10% of the spins in the system. This resonance is possibly an artifact brought about by the denaturation of the proteins upon freezing, whereby at least one of the heme ligands is displaced. The M7H spectrum shows a shoulder at $g \sim 6.3$, which becomes much more pronounced at pH 9 (data not shown). The LS resonances of wt cytochrome b_{562} H63N and M7H are listed in Table 1. The $g_{z,y}$, of wt and H63N are indistinguishable and are almost identical to those of M7H. The resonances are also similar to those of bis-imidazole-ligated hemin in solution (bis-Im-heme), which are also shown in the table. A precise g_x value for either cytochrome was difficult to determine because of the weak and broad nature of this feature; therefore, g_x values of 1.40 and 1.41 were calculated for H63N and M7H, respectively, by the method of Walker et al. (*17*) as described in the Materials and Methods.

Redox Potentiometry. The redox properties of the hemin-reconstituted H63N and M7H mutants and also bis-Im-heme were examined by redox potentiometry, and the redox titration curves are shown in Figure 5A. The H63N mutation has no effect on the midpoint potential, but the conversion of the heme-ligating methione to a His reduced the midpoint potential of the M7H cytochrome by 260 mV from +187 mV to −73 mV at pH 7.0. Despite this, the E_{m7} of M7H is 70 mV more positive than that of bis-Im-heme (−143 mV). Assuming that bis-Im-heme obeys a redox Bohr effect of −60 mV/pH unit (1 electron/1 proton), then the E_{m7} that we have measured is in good agreement with the $E_{m8.5}$ of −235 mV measured for bis-Im-heme previously (*23*).

The pH dependence of the M7H midpoint potential was examined, and the data are shown in Figure 5B. Similar data for the wt protein taken from ref *5* is also shown for comparison. The M7H data is fit to the following equation:

$$E = E_{low} + 59 \log \frac{[H^+] + K_{red}}{[H^+] + K_{ox}} \qquad (3)$$

where pK_{red} and pK_{ox} describe a protonation event when the heme is reduced and oxidized, respectively, and E_{low} is the E_m at pH $\ll$ pK_{ox} (*24*). The data were fit to pK_{red} = 6.8 and p$K_{ox} \ll 5$ (where the protein heme complex is not sufficiently stable to measure the E_m).

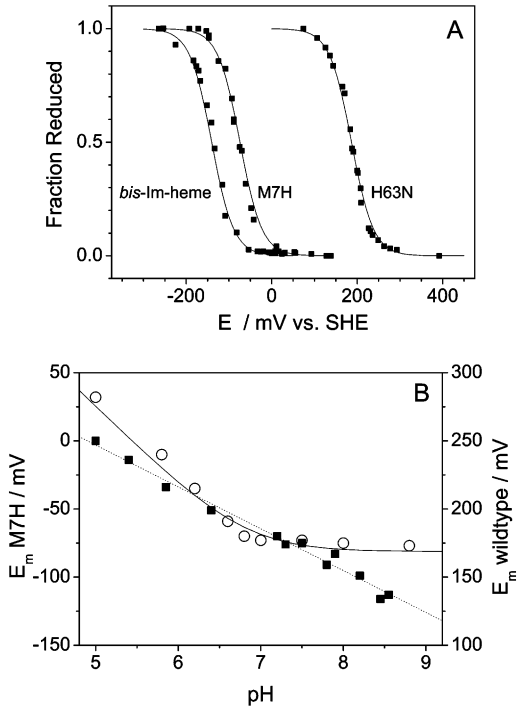

FIGURE 5: (A) Redox titration curves for bis-Im-heme and the hemin-reconstituted cytochrome b_{562} mutants M7H and H63N at pH 7.0. The fraction of reduced heme was determined by the change in Abs of the α band at ∼560 nm. The data are fit to a single Nernst curve with $n = 1.0$, and the midpoint potentials are given in Table 1. (B) pH dependence of the midpoint potential of M7H (○) fit to eq 3 with pK_{red} = 6.8 ± 0.1 and pK_{ox} fixed at 0. (■), Data for the wt taken from ref *5* and are fit to a line with a slope of −30 mV/pH unit.

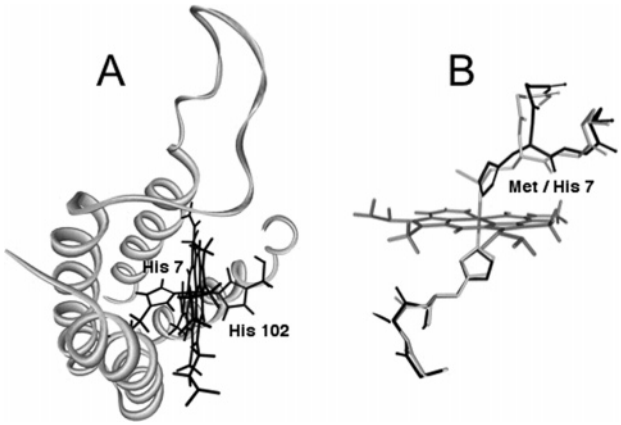

FIGURE 6: (A) Molecular model of the M7H mutant of cytochrome b_{562}. The model is an energy-minimized structure based on PDB file 256B created in HyperChem (Hypercube Inc.) using the Amber94 force field with a periodic box. (B) The heme-ligating side chains of M7H and wt cytochrome b_{562}. In gray is the coordinates from the wt protein. The two structures were aligned using the heme molecule. The backbone of the two amino acids on either side of Met/His 7 and His 102 are shown to highlight the perturbations that the M7H mutation is thought to create near His 7.

DISCUSSION

Molecular modeling of M7H suggests that the substitution of the heme-ligation Met at position 7 with His will disrupt the heme-binding pocket of the protein. Figure 6A shows a model of the mutant, and Figure 6B shows the disruption that the M7H mutation is thought to have on the heme-

binding site. The bulkier His is expected to disrupt the N-terminal α-helix around position 7. Additionally, the C-terminal helix is more disordered because of the movement of the heme to accommodate the additional His. Together, this will probably result in a more solvent-exposed heme. The modeling also indicates that the two His imidazole moieties will not be in-plane, and this is further discussed below with regard to the EPR data.

The far-UV CD spectra of apo and holo M7H (Figure 2) suggests that upon hemin binding less structural rearrangement occurs than in the wt. The solution structure of apocytochrome b_{562} shows that the C-terminal helix is largely unstructured (*4*) and, presumably, in the wt, helix formation only occurs upon heme binding. Gel-filtration chromatography shows that both apo and holo M7H have a larger hydrodynamic radius than H63N, suggesting a more disordered fold. However, as for the wt protein, there is a decrease in the apparent size of M7H upon hemin binding, which suggests that there is some conformational change. This may simply be due to the formation of the heme-His 102 ligation, which will anchor the C-terminal helix region of the protein. With the CD data, this suggests that there is little C-terminal helix formation in M7H upon heme binding, which will result in a potentially more solvent-exposed porphyrin and a less stable protein.

Thermal denaturation of apo-M7H and apo-wt cytochrome b_{562} occur with a similar ΔG (Table 3), suggesting that the N-terminal Met and H63N and M7H mutations do not significantly destabilize the apoprotein. There have been some differences in the reported chemical and thermal stabilities of holo-wt cytochrome b_{562} (*14*, *16*, *20*). The calculation of ΔG from thermal denaturation data requires an accurate ΔC_p value, and this may account for some of this disparity between values determined by thermal and chemical denaturation. The guanidine denaturation of ferri wt and ferri H63N yielded very similar ΔG values (7.0 and 6.8 kcal mol^{-1}) further confirming the minimal impact the H63N mutation has had on the stability of the cytochrome. The stability of holo M7H measured by both thermal and guanidine denaturation is in remarkably good agreement and shows only a small ∼1 kcal mol^{-1} stabilization of the protein upon heme binding. The difference in chemical stability between holo M7H and H63N was measured to be ∼2.5 kcal mol^{-1} [ΔG(H63N) = 6.8 kcal mol^{-1} and ΔG(M7H) = 4.3 kcal mol^{-1}]. It is reasonable to assume that this difference does not reflect the difference in bond strength between Met 7 S−Fe and His 7 N−Fe but rather that the M7H has disrupted hydrophobic contacts between the protein and the heme. The extent of the hydrophobic effect has been estimated to be ∼9.9 kJ/nm^2 of the water-excluded surface (*30*). The surface area of one side of a porphyrin is ∼1.0 nm^2; therefore, the difference in stability of H63N and M7H could be explained by the heme in M7H having additionally one-half of one side of the porphyrin solvent exposed relative to H63N (if the side chains also become solvent-exposed), and this could be achieved by the disruption of heme contacts of only two or three side chains in the binding pocket. This is consistent with the model of M7H (Figure 6), and it seems that the difference in stability between holo H63N and M7H is likely due to the disruption of the residues on either side of postion 7 and/or the disruption of heme contacts in the C-terminal helix. Interestingly, M7A mutants of the wt protein have been created, and these bind HS (5-coordinate) heme through His 102 with the ΔG^{H_2O} of the holo- and apoprotein very similar ($\Delta\Delta G \sim {}^1/_2$ kcal mol^{-1}) (*27*, *28*). This suggests that once the Met ligand in the wt protein is displaced, then the His-bound heme offers little additional stability to the protein. It also appears that bis-His ligation of heme in M7H offers little additional stability to the protein relative to ligation by a single His.

The difference in stability of the oxidized and reduced holocytochrome is directly related to the difference in redox potential (ΔE_f) between the folded (Table 1) (E_F) and unfolded (E_U) protein (reviewed in ref *31*). As an exposed heme in solution, i.e., E_f has a midpoint of about −100 mV (*31*, *32*), in the wt cytochrome b_{562}, ΔE_f is ∼300 mV, and thus, $\Delta\Delta G \sim 7$ kcal mol^{-1}. This difference in stability has been observed (*16*). The difference in the stability between ferri and ferrous M7H should be much smaller as $E_F \sim E_U$, and this was confirmed by thermal denaturation, where no significant difference in ΔG between oxidized and reduced holo M7H was observed.

Ferric and ferrous heme binding to apo M7H was measured to occur with K_d values of <1 and 20 nM, respectively. Conversely, binding to apo H63N occurred with K_d values of 13 and 3 nM for ferric and ferrous heme, respectively. This reversal in affinity for ferric over ferrous heme binding to M7H is expected because in solution Fe^{III}−porphyrins generally bind imidazoles and basic pyridines more tightly than Fe^{II}−porphyrins (see ref *26* and references within). These values are only estimates because it is possible that they were not measured at equilibrium because of ferric or ferrous heme being kinetically trapped in either H63N or M7H in an analogous manner to that reported for cytochrome b_5 (*29*). Nevertheless, the M7H has altered the energetics of heme binding in a predictable fashion, and to our knowledge, this is the first example of a comparison between the heme-binding energetics in equivalent cytochromes with bis-His and His/Met ligation.

Both apo H63N and apo M7H can bind free-base protoporphyrin IX, which implies that the heme-binding pocket, i.e., those amino acids in the vicinity of the bound heme, is not seriously compromised by the M7H mutation and plays a role in heme binding. This suggests that the destabilization of holo M7H is due to subtle conformational changes that leave the binding pocket relatively intact. The experiments of Huffman et al. (*25*) showed that the presence of noncoordinating hydrophobic residues flanking the heme-binding His can increase heme binding to a synthetic peptide by >20 kJ mol^{-1} (4.8 kcal mol^{-1}). Because the differences between the energetics of binding of heme or hemin to H63N or M7H are probably smaller than this (<2 kcal mol^{-1}, Table 2), this also suggests that the heme-binding pocket is not significantly altered in M7H. The Soret-region CD spectra (Figure 2) of ferri and ferrous M7H are qualitatively similar to those reported for wt cytochrome b_{562} (*22*), and it is unlikely that this would be the case if the binding pocket in M7H was significantly altered.

The Abs spectra of oxidized and reduced M7H are not remarkable except for the unusually broad and partially split α band of ferrous M7H (Figure 1 and Table 1). Splitting of the α band is uncommon but is seen in the split α cytochromes (*33*). Such splitting was recently reported for a heme-ligating Met to His mutant of *Pseudomonas* cyto-

chrome c_{551} (*34*) and may be a characteristic of the perturbed ligand environment of Met to His cytochrome *b* mutants. Interestingly, no splitting of this α band has been reported for the synthetic heme-binding peptides of Dutton and others, yet these peptides are expected to have an unusual heme-binding environment (reviewed in ref *11*). We do not think that this splitting is due to heme orientation disorder, and no changes in the Abs spectra of freshly reconstituted holo M7H are observed on the minutes−days time frame. Rather, this splitting is probably due to asymmetry of the bound heme (for example, see ref *35*) perhaps because of iron movement out of the porphyrin plane or slight deformation of the porphyrin because of steric strain. The Abs bands of both ferri and ferrous M7H are blue-shifted relative to those of H63N. This is consistent with previous experiments, which have shown that axial ligation can shift the Abs maxima of bound heme. The *N*-acetylmethionine complex of ferric microperoxidase-8, which contains His/Met-ligated hemin, has a Soret Abs maxima 1.5 and 3.0 nm to the red of the respective *N*-acetylhistidine and imidazole complexes (*36*, *37*). An alternate explanation for these shifts is the observation that increasing the solvent polarity causes blue-shifting of the Abs maxima of model heme complexes (*38*). Thus, the shifts observed between M7H and H63N are probably due to both the different axial ligation and additional solvent exposure of heme in M7H.

The H63N and M7H EPR data (Figure 4) are very similar and consitant with the hemin in a predominantly LS 6-coordinate configuration. Both spectra show some HS signal at $g \sim 5.9$, which is probably due to freezing-induced dissociation of the heme from the cytochrome. However, the M7H spectrum has some broadening and splitting of the heme $g \sim 5.9$ resonance, which becomes much more pronounced at pH 9 (not shown). This splitting has been attributed to the paramagnetic electron no longer having equal interaction with the four nitrogen atoms of the porphyrin (i.e., the porphyrin ring is no longer planar) and is observed in some HS globins and cytochromes (*39*). This would suggest that the HS heme is still bound to M7H and is nonplanar. There is no evidence of HS M7H-bound hemin at room temperature, because there are no typical HS Abs peaks, but it is interesting to speculate that the M7H mutation may place the bound heme under some steric strain. This could account for the split α Abs band of ferrous M7H. Using the measured LS g_z, g_y, and calculated g_x tensors of H63N and M7H (Table 1), the rhombic and tetragonal splittings were calculated with $V/\lambda = 1.60$ and 1.64 and $\Delta/\lambda = 3.37$ and 3.27, respectively. When these are plotted by the method of Peisach et al. (*39*) as rhombicity (V/Δ) versus tetragonal field (Δ/λ), they both fall within the H group of heme EPR spectra, which is assigned to ligation of the heme iron by two His iminonitrogens. This is obviously not the case for H63N. Interestingly the M7H V/λ value of 1.64 is considerably less than $V = 2\lambda$ (which occurs when the two His imidazole groups are parallel to each other), suggesting that the orientation of the two ligating His imidazole planes is somewhat twisted relative to each other and is in agreement with the molecular model of Figure 6.

It has been experimentally shown that heme bound through His/Met ligation has a midpoint potential of ∼150 mV more positive than its bis-His equivalent (*40*). This difference is due to the greater electron-withdrawing ability of the Met sulfur, which destabilizes the positively charged oxidized heme. This effect is exemplified in the *c*-type cytochromes, where the redox potentials of His/Met and bis-His-ligated heme range between 0 to +400 and −400 to −100 mV, respectively (reviewed in ref *41*). In addition, this effect is additive because H102M mutants of cytochrome b_{562}, which bind heme through bis-Met ligation, have midpoint potentials about 180−200 mV higher than the wt cytochrome (*6*). The ΔE_{m7} of M7H versus H63N (Figure 5A and Table 1) is 260 mV, ∼100 mV greater than the 150 mV predicted (*40*). rCDH, the only other known *b*-type cytochrome with His/Met ligation, has an $E_{m4.5}$ of +164 mV, while the bis-His mutant of this protein has an $E_{m4.5}$ of −53 mV (*2*). This ΔE_m of 217 mV is more similar to that observed for wt and M7H cytochrome b_{562} than that suggested by model compounds (*40*). The bis-His mutant of rCDH has unusual ligation through His imidazole $N^{\delta 1}$ and $N^{\epsilon 2}$ nitrogens. This form of ligation is very rare but is observed in one of the four hemes of cytochrome c_{554} from *Nitrosomonas europaea*. This heme has been assigned an unusually high (for bis-His ligation) midpoint potential of +47mV (*42*), and it seems that N^{ϵ}/N^{δ}-ligated heme can have a higher midpoint potential than an equivalent N^{ϵ}/N^{ϵ}-ligated heme (see ref *42* for a discussion of this). While this type of ligation cannot be ruled out in M7H, there are other explanations as to why there is such a large difference in midpoint potentials between H63N and M7H. One explanation for this is consistent with the observation that the M7H mutation leaves the bound heme more solvent-exposed than in the wt. It has been experimentally shown using synthetic heme-binding peptides that the protein hydrophobicity can exert a ±∼50 mV effect on the heme redox potential (*43*), but this presumably accounts for at least some of the 70 mV difference between the E_{m7} of bis-imidazole and M7H-ligated heme. The difference in K_d values for ferric and ferrous heme-binding to H63N and M7H (Table 2) will play a role in the difference in midpoint potentials (ΔE_m) between these two cytochromes. The stability of ferric over ferrous heme binding in M7H stabilizes the oxidized state by at least ∼1.7 kcal mol^{-1} or 75 mV (see ref *44* for a complete description of this effect). Similarly, the difference in binding energetics in H63N also contributes to this, and ΔE becomes ∼110 mV between M7H and H63N because of this preferential binding. The magnitude of this effect can account for the unexplained difference between the ΔE_m of H63N and M7H, but it should be stated that some of the 150 mV difference between the ΔE_m of His/Met and bis-His-ligated heme observed by Harbury and Loach (*40*) can probably also be explained by this argument. A range of midpoint potentials spanning >160 mV was observed in a library of *in vitro*-evolved cytochrome b_{562} variants (*8*, *45*). In 2 generations of mutants, which all maintained His/Met heme ligation, only one mutant displayed a midpoint potential more positive than the wt protein. This led the authors to suggest that cytochrome b_{562} has evolved to have a midpoint potential at the positive extreme allowed by the architecture of the protein, and almost any alteration to the protein will lower this potential. Thus, the M7H mutation, which has a potential in the upper range of bis-His-ligated cytochromes, is expected to disrupt some of the mechanisms that cytochrome b_{562} has perfected to produce the most positive midpoint potential that the protein architecture will allow. This will result in a lowering of the

midpoint of M7H through protein−porphyrin interactions in addition to those manifested through the axial ligands.

The pH dependence of the midpoint potential of M7H is dominated by a single ionization in the reduced state (Figure 5B). A pK of 6.8 has previously been assigned to a heme propionate in wt cytochrome b_{562} by using NMR chemical shifts (*5*), and this propionate is most likely the ionizable group responsible for the pK_{red}. The pH dependence of the wt E_m is unusual with a approximately linear dependence with a slope of ∼30 mV per pH unit. The pH dependence from pH 5.0 to 8.5 has been described as arising from at least 5 single proton ionizations including both heme propionates (*5*). Direct electrochemistry of cytochrome b_{562} gave similar results (*46*), and the authors fit their data to two pK_{red} and two pK_{ox}. The data for M7H do not contain enough data points to reliably exclude other pK_{red} and pK_{ox} events, but the dominance of the single propionate on the measured E_m is evident. One of the ionizable groups in the wt cytochrome b_{562} is probably His 102, which appears to get deprotonated at an unusually low pH (pK_a ∼ 9) because of the stabilization of the histidinate anion by arginine 98 and 106 (*5*). This appears to be disrupted in M7H, where presumbably this stabilization is lost and the pK_a of His 102 becomes >9. This is consistent with structural pertubation of the C-terminal helix as previously suggested but could also be achieved through a relatively small twist of the plane of the imidazole of His 102, which is consistent with EPR. Interestingly, the bis-Met mutants of cytochrome b_{562} have a qualitatively similar E_m pH dependence as the wt protein described by two of each pK_{red} and pK_{ox} events (*46*). These mutants were generated by replacing the His at position 102 and indicate that other ionizable groups play a significant role in the unusual pH behavior of the redox properties of the wt cytochrome b_{562}.

Many of our arguments could be resolved by knowledge of the structure of the M7H cytochrome; therefore, we are currently attempting to crystalize this protein for X-ray diffraction. We have generated small crystals thus far, which although are too small for measurements, give us hope that the protein is reasonably well-structured and has a dominant conformer. The M7H mutant cytochrome that we have described is a small, soluble, single-heme-binding protein. With bis-His ligation, the protein becomes a good minimalistic example of a typical *b*-type cytochrome.

ACKNOWLEDGMENT

We thank Karin Ahrling for assistance with EPR measurements and Reza Razeghifard for useful discussions.

REFERENCES

1. Itagaki, E. and Hagar, L. P. (1966) Studies on cytochrome b_{562} of *E. coli*. Purification and crystallization of cytochrome b_{562}, I. *J. Biol. Chem. 241*, 3687−3695.
2. Rotsaert, F. A. J., Hallberg, B. M., de Vries, S., Moenne-Loccoz, P., Divne, C., Renganathan, V., and Gold, M. H. (2003) Biophysical and structural analysis of a novel heme b iron ligation in the flavocytochrome cellobiose dehydrogenase, *J. Biol. Chem. 278*, 33224−33231.
3. Hamada, K., Bethge, P. H., and Mathews, F. S. (1995) Refined structure of cytochrome b_{562} from *Escherichia coli* at 1.4 Å resolution, *J. Mol. Biol. 247*, 947−962.
4. Arnesano, F., Banci, L., Bertini, I., Faraone-Mennella, J., Rosato, A., Barker, P. D., and Fersht, A. R. (1999) The solution structure of oxidized *Escherichia coli* cytochrome b_{562}, *Biochemistry 38*, 8657−8670.
5. Moore, G. R., Williams, R. J. P., Peterson, J., Thomson, A. J., and Mathews, F. S. (1985) A spectroscopic investigation of the structure and redox properties of *Escherichia coli* cytochrome b_{562}, *Biochim. Biophys. Acta 829*, 83−96.
6. Barker, P. D., Nerou, E. P., Cheesman, M. R., Thomson, A. J., de Oliveira, P., and Hill, H. A. (1996) Bis-methionine ligation to heme iron in mutants of cytochrome b_{562}. 1. Spectroscopic and electrochemical characterization of the electronic properties, *Biochemistry 35*, 13618−13626.
7. Robinson, C. R., Liu, Y., Thomson, A. J., Sturtevant, J. M., and Sligar, S. G. (1997) Energetics of heme binding to native and denatured cytochrome b_{562}, *Biochemistry 36*, 16141−16146.
8. Springs, S. L., Bass, S. E., Bowman, G., Nodelman, I., Schutt, C. E., and McLendon, G. L. (2002) A multigeneration analysis of cytochrome b_{562} redox variants: Evolutionary strategies for modulating redox potential revealed using a library approach, *Biochemistry 41*, 4321−4328.
9. Razeghifard, M. R., and Wydrzynski, T. (2003) Binding of Zn-chlorin to a synthetic four-helix bundle peptide through histidine ligation, *Biochemistry 42*, 1024−1034.
10. Teale, F. W. F. (1959) Cleavage of haem−protein link by acid methylethyl ketone, *J. Biochim. Biophys. Acta 35*, 543.
11. Gibney, B. R., and Dutton, P. L. (2001) *De novo* design and synthesis of heme proteins, in *Advances in Inorganic Chemistry* (Mauk, A. G, and Sykes, A. G., Eds.) Vol. 51, pp 409−455, Academic Press, New York.
12. Lombardi, A., Nastri, F., Pavone, V. (2001) Peptide-based heme−protein models, *Chem. Rev. 101*, 3165−3189
13. Pace, C. N. (1986) Determination and analysis of urea and guanidine hydrochloride denaturation curves, *Methods Enzymol. 131*, 266−280.
14. Robinson, C. R., Liu, Y., O'Brien, R., Sligar, S. G., and Sturtevant, J. M. (1998) A differential scanning calorimetric study of the thermal unfolding of apo- and holo-cytochrome b_{562}, *Protein Sci. 7*, 961−965.
15. Dutton, P. L. (1978) Redox potentiometry: Determination of midpoint potentials of oxidation−reduction components of biological electron-transfer systems, *Methods Enzymol. 54*, 411−435.
16. Wittung-Stafshede, P., Gray, H., and Winkler, J. R. (1997) Rapid formation of a four-helix-bundle, Cytochrome b_{562} folding triggered by electron transfer, *J. Am. Chem. Soc. 119*, 9562−9563.
17. Walker, F. A., Huynh, B. H., Scheidt, W. B., and Osvath, S. R. (1986) Models for cytochromes *b*. Effect of axial ligand plane orientation on the EPR and Mössbauer spectra of low-spin ferrihemes, *J. Am. Chem. Soc. 108*, 5288−5297.
18. Taylor, C. P. S. (1977) The EPR of low spin heme complexes, *Biochim. Biophys. Acta 491*, 137−149.
19. Eaton, W. A., and Hochstrasser, R. M. (1967) Electronic spectrum of single crystals of ferricytochrome-*c*, *J. Phys. Chem. 46*, 2533−2539.
20. Feng, Y. Q., and Sligar, S. G. (1991) Effect of heme binding on the structure and stability of *Escherichia coli* apocytochrome b_{562}, *Biochemistry 30*, 10150−10155.
21. Zhou, N. E., Kay, C. M., and Hodges, R. S. (1992) Synthetic model proteins. Positional effects of interchain hydrophobic interactions on stability of two-stranded α-helical coiled-coils, *J. Biol. Chem. 267*, 2664−2670.
22. Bullock, P. A., and Myer, Y. P. (1978) Circular dichroism and resonance Raman studies of cytochrome b_{562} from *Escherichia coli*, *Biochemistry 17*, 3084−3091
23. Shifman, J. M., Gibney, B. R., Sharp, R. E., and Dutton, P. L. (2000) Heme redox potential control in *de novo* designed four-α-helix bundle proteins, *Biochemistry 39*, 14813−14821.
24. Clarke, W. M. (1960) *Oxidation−Reduction Potentials of Organic Systems*, Bailliere, Tindall, and Cox, Ltd., London, U.K.
25. Huffman, D. L., and Suslick, K. S. (2000) Hydrophobic interactions in metalloporphyrin−peptide complexes, *Inorg. Chem. 39*, 5418−5419.
26. Nesset, M. J. M., Shokhirev, N. V., Enemark, P. D., Jacobson, S. E., and Walker, F. A. (1996) Models of the cytochromes. Redox properties and thermodynamic stabilities of complexes of hindered iron(III) and iron(II) tetraphenylporphyrinates with substituted pyridines and imidazoles, *Inorg. Chem. 35*, 5188−5200.
27. Kamiya, N., Okimoto, Y., Ding, Z., Ohtomo, H., Shimizu, M., Kitayama, A., Morii, H., and Nagamune, T. (2001) How does axial ligand deletion affect the structure and the function of cytochrome b_{562}? *Protein Eng. 14*, 415−419.
28. Uno, T., Yukinari, A., Moriyama, Y., Ishikawa, Y., Tomisugi, Y., Brannigan, J. A., and Wilkinson, A. J. (2001) Engineering a

ligand binding pocket into a four-helix bundle protein cytochrome b_{562}, *J. Am. Chem. Soc. 123*, 512−513.
29. Altuve, A., Silchenko, S., Lee, K.-H., Kuczera, K., Terzyan, S., Zhang, X., Benson, D. R., and Rivera, M. (2001) Probing the differences between rat liver outer mitochondrial membrane cytochrome b_5 and microsomal cytochromes b_5, *Biochemistry 40*, 9469−9483.
30. Chothia, C. (1974) Hydrophobic bonding and accessible surface area in proteins, *Nature 248*, 338−339.
31. Mines, G. A., Pascher, T., Lee, S. C., Winkler, J. R., and Gray, H. B. (1996) Cytochrome *c* folding triggered by electron transfer, *Chem. Biol. 3*, 491−497.
32. Bixler, J., Bakker, G., and McLendon, G. (1992) Electrochemical probes of protein folding, *J. Am. Chem. Soc. 114*, 6938−6939.
33. Meyer, T. E., and Kamen, M. D. (1982) New perspectives on *c*-type cytochromes, *Adv. Protein Chem. 35*, 105−212.
34. Miller, G. T., Zhang, B., Hardman, J. K., and Timkovich, R. (2000) Converting a *c*-type to a *b*-type cytochrome: Met61 to His61 mutant of *Pseudomonas* cytochrome *c*551, *Biochemistry 39*, 9010−9017.
35. Reddy, K. S., Angiolillo, P. L., Wright, W. W., Laberge, M., and Vanderkooi, J. M. (1996) Spectral splitting of the $\alpha(Q_{0,0})$ absorption band of ferrous cytochrome *c* and other heme proteins, *Biochemistry 35*, 12820−12830.
36. Othman, S., Le Lirzin, A., and Desbois, A. (1994) Resonance Raman investigation of imidazole and imidazolate complexes of microperoxidase: Characterization of the bis(histidine) axial ligation in *c*-type cytochromes, *Biochemistry 33*, 15437−15448.
37. Othman, S., and Desbois, A. (1998) Resonance Raman investigation of lysine and *n*-acetylmethionine complexes of ferric and ferrous microperoxidase, *Eur. Biophys. J. 28*, 12−25.
38. Romberg, R. W., and Kassner, R. J. (1982) Effects of solvent on the absorption maxima of five-coordinate heme complexes and carbon monoxide-heme complexes as models for the differential spectral properties of hemoglobins and myoglobins, *Biochemistry 21*, 880−886.
39. Peisach, J., Blumberg, W. E., and Adler, A. (1973) Electron paramagnetic resonance studies of iron porphyrin and chlorin systems, *Ann. N.Y. Acad. Sci. 206*, 310−327.
40. Harbury, H. A., and Loach, P. A. (1960) Oxidation-linked proton functions in heme octa- and undecapeptides from mammalian cytochrome *c*, *J. Biol. Chem. 235*, 3640−3645.
41. Moore, G. R., and Pettigrew, G. W., Eds. (1990) *Cytochromes c. Evolutionary, Structural, and Physicochemical Aspects*, Springer−Verlag, Berlin, Germany.
42. Upadhyay, A. K., Petasis, D. T., Arciero, D. M., Hooper, A. B., Hendrich, M. P. (2003) Spectroscopic characterization and assignment of reduction potentials in the tetraheme cytochrome c_{554} from *Nitrosomonas europaea*, *J. Am. Chem. Soc. 125*, 1738−1747.
43. Gibney, B. R., Huang, S. S., Skalicky, J. J., Fuentes, E. J., Wand, A. J., and Dutton, P. L. (2001) Hydrophobic modulation of heme properties in heme protein maquettes, *Biochemistry 40*, 10550−10561.
44. Kennedy, M. L., Silchenko, S., Houndonougbo, N., Gibney, B. R., Dutton, P. L., Rodgers, K. R., and Benson, D. R. (2001) Model hemoprotein reduction potentials: The effects of histidine-to-iron coordination equilibrium, *J. Am. Chem. Soc. 123*, 4635−4636.
45. Springs, S. L., Bass, S. E., and McLendon, G. L. (2000) Cytochrome b_{562} variants: A library for examining redox potential evolution, *Biochemistry 39*, 6075−6082.
46. Barker, P. D., Butler, J. L., De Oliveira, P., Hill, H. A. O., and Hunt, N. I. (1996) Direct electrochemical studies of cytochromes b_{562}, *Inorg. Chim. Acta 252*, 71−77.
47. John, D. M., and Weeks, K. M. (2000) van't Hoff enthalpies without baselines, *Protein Sci. 9*, 1416−1419.

BI0492298